Comparison of three different methodologies for the identification of high atmospheric turbidity episodes

D. Mateos[1], V. E. Cachorro[1], C. Velasco-Merino[1], N. T. O'Neill[2], M.A. Burgos[1], R. Gonzalez[1], C. Toledano[1], M. Herreras[1], A. Calle[1], A.M. de Frutos[1]

[1] GOA, Departamento de Física Teórica, Atómica y Óptica, Facultad de Ciencias, Universidad de Valladolid, Paseo Belén 7, 47011, Valladolid, Spain.

[2] CARTEL, Université de Sherbrooke, Sherbrooke, Québec, Canada

Abstract

The identification and characterization of High Atmospheric Turbidity (HAT) episodes is a key objective of global aerosol monitoring. This study presents a comparison of three different methodologies that were used to identify HAT episodes in the north-central Iberian Peninsula. The first methodology (named C&S inventory) is based on columnar aerosol optical depth (AOD from the Aerosol Robotic Network, AERONET) and surface particulate matter concentrations (PMx from the European Monitoring and Evaluation Programme, EMEP) as well as ancillary information. Another methodology (named SPR) is based on PM surface concentrations levels and ancillary information. Both methods are carefully reviewed by human observers. A third method, based only on fine and coarse mode values of AOD was also analysed. This method (the SDA or Spectral Deconvolution Algorithm) is found to be a good operational candidate for automating the identification of HAT episodes. The three methods allow for the identification of mineral desert dust (coarse type 'D') aerosols and aerosols of fine type, 'A' (i.e. biomass burning or polluted aerosols): their mixture, categorized as 'MD' and 'MA' classes (depending of the prevailing 'D' or 'A' type) is only identified in the C&S and SDA inventories. The three inventories show about 60% coincidence across a 2005-2014 reference period. When the C&S and SDA inventories are compared, the agreement is very high if columnar aerosol data is available: >90% for desert aerosol type and >70% for fine aerosol type. The comparative study of these three aerosol inventories was motivated by the need to automate existing methodologies.

Keywords: high turbidity episodes; columnar and surface aerosols; desert dust; biomass burning urban industrial; coarse and fine modes;

Nomenclature

α: spectral derivative of AOD at 500 nm

α': Spectral derivative of α

A: Flag for pollution caused by urban-industrial and biomass burning aerosols

AE: Ångström exponent

AOD: Aerosol Optical Depth

AOD_{500}: Aerosol Optical Depth at 500 nm

AOD_C: Coarse mode Aerosol Optical Depth at 500nm

AOD_F: Fine mode Aerosol Optical depth at 500nm

C: Flag for pollution caused by coarse aerosols (only in SDA inventory)

C&S: 'Columnar and Surface' inventory

D: Flag for pollution caused by mineral dust aerosols

DS: Direct Sun products from AERONET network

η: fine mode fraction (at 500 nm)

F: Flag for pollution caused by fine aerosols (only in SDA inventory)

HAT: High atmospheric turbidity

M: Flag for pollution caused by a mixture of fine and coarse aerosols (only in SDA inventory)

MA: Flag for a pollution mixture with predominance of urban-industrial and biomass burning aerosols

MD: Flag for a pollution mixture with predominance of mineral dust aerosols

NT: Flag for non-turbid cases (only in SDA inventory)

SDA: 'Spectral Deconvolution Algorithm' inventory

SPR: 'Spanish and Portuguese Reference method' inventory

1. Introduction

Atmospheric aerosols represent a large source of uncertainty in the complex Earth-atmosphere climate system. They have a notable impact on critical issues such as the radiative budget, air quality, human health, hydrological cycle, cloud life cycle, etc.(e.g., Boucher et al., 2013). The contribution of aerosols to these effects is magnified during high atmospheric turbidity (HAT) episodes: strong aerosol loads that occur over large, regional, or local scales and over short time periods. Aerosols from distant or nearby emission sources can, during HAT episodes, dramatically change the typical values observed for aerosol load levels in a given area as well as their optical and microphysical properties. Aerosol characterization during such HAT episodes can be accomplished using different measuring techniques. For air quality monitoring, PM_{10} (particulate matter concentration for particle sizes below 10 μm in diameter) or speciation measurements are used to detect those days with concentration data in excess of the established safety thresholds for human health (e.g., Pey et al. 2013, using European Monitoring and Evaluation Programme, EMEP, data). Networks of ground-based data using Sun photometers or Lidar instruments, such as AERONET (AERosol Robotic NETwork, Holben et al., 1998) and EARLINET (European Aerosol Research Lidar Network, Pappalardo et al., 2014), can provide regional to global-scale indicators of HAT episodes. Furthermore, satellite observations provide data for wider interpretation of global scale phenomena (e.g., CALIOP-CALIPSO, MODIS) (e.g., Levy et al., 2010).

Recent studies have demonstrated the relevance of long-term identification and characterization of different HAT episodes (e.g., Toledano et al., 2007; Valenzuela et al., 2012; Gkikas et al., 2013, 2016a; Pey et al., 2013; Burgos et al., 2016). Columnar quantities such as Aerosol Optical Depth (AOD) and the Ångström Exponent (AE), defined by the spectral slope of the AOD across a given wavelength interval, are commonly used in the discrimination of aerosol types: these being mainly, maritime, desert dust, urban, biomass burning, and mixtures (e.g., Holben et al., 2001; Toledano et al., 2007; Bennouna et al., 2016). A simple scattergram plot of AE vs AOD enables certain thresholds to be defined in order to discriminate aerosol types. The use of air mass back trajectories allows the identification of aerosol sources (e.g., Pace et al., 2006; Valenzuela et al., 2012) and is accordingly, a key source of information for aerosol type identification. Similar methods have been recently applied to satellite data to identify and characterize different aerosol types over large areas (e.g., Gkikas et al., 2016a, 2016b). These methods differ in the selected aerosol parameter/properties (such as fine mode fraction, effective radius, among others) and threshold values. However, the weakness of these methods is that generally they are only efficient for identifying relatively strong episodes in terms of AOD values.

The lack of studies comparing different methodologies whose nominal mandate is the identification of aerosol episodes, underscores the need for more exhaustive analyses of this nature. Hence, this study presents a comprehensive comparison between three different HAT identification techniques that employ columnar and/or surface data. Cachorro et al. (2016) developed a long-term (2003 to 2014) desert dust inventory over north-central Spain based on the visualization and analysis of both surface and columnar aerosol data together with other ancillary information. This methodology is also employed in this study (with some adaptations) to identify HAT episodes related to the incursion of urban-industrial and biomass burning aerosols and other fine mode dominated aerosols. This day-by-day visualization of an entire data series over a certain site can be considered the most comprehensive way to address the issue of HAT event day identification, and constitutes our first inventory. The handicap of such careful monitoring is that the process cannot easily be applied to a large area with many measurement stations. Moreover, long-term datasets often have missing data for extended periods of time. This lack of measurements may prevent from appropriate detection of HAT episodes. Given the strong seasonality of long-range transported aerosol events, the absence of data in certain periods or seasons can also affect the overall statistics. The combination of columnar and in situ aerosol data is therefore helpful to minimize the gaps in the analysis.

A second inventory is performed every year by the Spanish Government using weather forecasts, aerosol model forecasts and a re-evaluation of the inventory with surface PM concentrations in different sectors of the Iberian Peninsula (Viana et al., 2010; MITECO, 2019). These two methods must be carried out by human observers with considerable expertise and can require significant time to be completed. They are difficult to apply in real time over large areas with many sites. Indeed, a bibliographic search indicated that no real time reference method is currently available. For these reasons a new automatic method, requiring only aerosol columnar data, is proposed and applied in this study. This third inventory method, applied for the first time as part of this study, detects the occurrence of coarse and/or fine mode HAT event days.

The very clean background over the plateau of the north-central Iberian Peninsula enables an accurate identification of different types of HAT episodes. The closeness to the African continent ensures that desert dust aerosol will be one of the most dominant aerosol types throughout the year. Urban-industrial and biomass burning aerosols are also present due to local sources as well as long range transport from European and North American sources. The complex orography of the Iberian Peninsula also ensures extended periods of air mass recirculation and therefore the observation of aged aerosol, particularly during the summer months.

The aim of this study is to carry out a comprehensive comparison among the three above-mentioned methodologies for identifying high atmospheric turbidity event days in the central area of the Iberian Peninsula between 2005 and 2014. For illustration, the identification of all the episodes registered during the entire year 2014 is presented as a particular case study. Furthermore, the sensitivity of the proposed automated method to the threshold selection is also investigated.

2. Aerosol Database

2.1. Columnar AERONET and surface EMEP aerosol data

Columnar aerosol data presented in this study are measured using the CIMEL CE-318 Sun photometers (Holben et al., 1998; Giles et al., 2019) at the Palencia site (41.9º N, 4.5º W, and 750 m a.s.l.) belonging to AERONET/RIMA (AERosol RObotic NETwork/ "Red Iberica de Medida fotométrica de Aerosoles") since 2003. Direct sun (DS) data include spectral AOD_{DS} at 7 different wavelengths (340, 380, 440, 500, 675, 870, 1020 nm respectively) and the associated Ångström Exponent (AE_{DS}) retrieved from the AOD using different pairs (or intervals) of wavelengths (Vergaz et al., 2001). These 15-minute daytime records (level 1.0) are processed under cloud-screening algorithm (level 1.5) and they are considered as 'instantaneous values' which can be used to identify changes of aerosol properties across very small time scales. All these records are also daily averaged to characterize day to day statistics. The 'instantaneous' or daily averaged databases are used depending on the case. Only AERONET version 2 level 2 (quality assured) DS products between 2003 and 2014 were analyzed. The data coverage in this period for the sun photometer is 67% (for AOD), and the EMEP data coverage is 90% (for PM_{10}). For further details and year-to-year information, see Cachorro et al. (2016).

With respect to aerosol surface concentration measurements, the closest site to Palencia is a rural site located at Peñausende (41.28ºN, 5.87ºW, and 985 m a.s.l.), belonging to the EMEP (European Monitoring and Evaluation Programme) network. Daily sampled PM_{10} particle concentrations are obtained by gravimetric determinations. These high quality measurements are the official data reported to the European Commission (e.g., Pey et al., 2013). These PM_{10} data started in year 2000. The distance of 100km between Palencia (columnar data) and Peñausende (surface data) does not introduce any effect regarding the identification of HAT event days (Cachorro et al., 2016).

2.2. AERONET SDA collection data

AERONET provides a high number of aerosol products derived from different algorithms which use different inputs (direct sun, sky radiance measurements, AOD data, etc.). In particular, the Spectral

Deconvolution Algorithm (SDA ; O'Neill et al., 2001, 2003) algorithm employed by AERONET utilizes as input five spectral AOD values in the 380-870 nm spectral range. The output is a variety of fine and coarse mode products (see Section 3.2). Those products are evaluated at a reference wavelength of 500 nm, and include: total AOD at 500nm (named AOD_{500} as mentioned above), fine mode AOD (AOD_F) and coarse-mode AOD (AOD_C), fine mode fraction ($\eta=AOD_F/AOD$), spectral AOD derivative (α, as per O'Neil et al., 2001), and spectral derivative of α, denoted as α'. Here, we must note the different meaning of α and AE, both are defined in the literature as the Ångström coefficient, but α is defined as the spectral derivative of AOD at a specific wavelength (500 nm in the SDA algorithm) and AE is related with a given spectral wavelength interval. More details about these concepts were given by Shifrin (1995). Therefore the values of α and AE are different but a strong correlation exists between both coefficients.

The AERONET version 2 level 2 (quality-assured) SDA product is only available since July 2008 at Palencia site. To extend the analysis between 2005 and 2008, an extra quality control was applied to level 1.5 data to ensure data and retrieval SDA reliability. We were able to extend our analysis to the entire 2005-2014 period. A few details concerning the nomenclature are worth to be mentioned: the DS algorithm AODs used throughout the text are those derived at the 440 nm channel and always appear with the subscript 'DS' (see first paragraph of Section 2), while the SDA retrievals are subscript-free and referenced to a wavelength of 500 nm.

Based on these measured/derived data, three different inventories have been constructed. The inventory named "SPR" (see Section 3.3) uses only surface PM_{10} data; and the "SDA" inventory uses only columnar AOD data (see Section 3.2). The inventory named "C&S" (see Section 3.1) uses both columnar AOD_{DS} at 440 nm ($AOD_{DS,440nm}$) and surface PM_{10} data. The common database with both columnar and surface aerosol data used in this study spans between 2005 and 2014.

2.3. Ancillary information: HYSPLIT model

Air mass back-trajectories of 120 hours duration were calculated with the version 4 HYSPLIT model (Hybrid Single-Particle Lagrangian Integrated Trajectory; Stein et al., 2015) at 8, 12 and 16 UTC, and at six atmospheric heights (500, 1500, 3000, 4000, 5500, and 7000 m a.g.l.) in order to check the trajectory of the air masses and therefore the possible aerosol sources during HAT episodes. The six heights were chosen to accommodate the fact that the transport of particles associated with high turbidity episodes

can occur at altitude levels below and above the boundary layer. The evaluation of the air mass trajectories is carried out at three different times each day in an attempt to account for different diurnal variants of HAT occurrence. This includes when a HAT episode is starting/ending. During these initial or final periods, the HAT conditions can occur only in just a few hours of the whole day. The meteorological database used as input for HYSPLIT is the Global Data Assimilation System (GDAS) dataset. HYSPLIT-derived sources were defined when the air masses spent at least 15% of the entire back-trajectory (at any height) over Africa, Europe, Mediterranean Basin, American Continent, Atlantic Ocean, and locally (Iberian Peninsula). Further details of the followed methodology were explained in detail by Mateos et al. (2015). In this study, the air mass back-trajectories were, in particular, employed to corroborate the presence of mineral dust, urban-industrial and biomass burning aerosols.

3. Methods for identifying high atmospheric turbidity conditions

The methods presented in this study allows discriminating between two main types of HAT episodes: those related to coarse mode mineral dust, and those related to fine particles whose origin can mostly be attributed to anthropogenic sources and biomass burning. Desert dust outbreaks will be identified with a 'D' flag. The 'A' flag includes mainly fine mode aerosols resulting from fossil fuel combustion from industry or urban-pollution, biomass burning (BB) aerosols from forest fires and other atmospheric processes, mainly of anthropogenic origin. However, this well-defined coarse and fine particle types are usually mixed with variable fine/coarse mode contribution, giving rise to aerosol mixtures. We have distinguished two of them, 'MD' and 'MA', to indicate that desert dust or fine aerosol particles are predominant in that aerosol mixture, respectively. These cases of mixtures are only distinguished in the C&S and SDA methodologies (see below).

We must note that episodes dominated by fine mode particles represent aerosols of different type which are difficult to distinguish because of the necessity of other more specific parameters (i.e., absorption coefficient or single scattering albedo in the case of columnar aerosol measurements or speciation in the case of PM_{10} filter measurements). However, given the clean atmospheric characteristic of our area of study, BB and pollution aerosol episodes can be easily distinguished by analysing ancillary information, such as air mass back-trajectories and public domain information (e.g. newspaper information about local or strong regional forest fires).

We also must emphasize that the existing methodologies to detect and evaluate the episodes of HAT are not simple, because they require different data and information of different sources to give reliable results. and they are time-consuming and rely on the researcher expertise. Therefore, novel automatic

methodologies as proposed in this paper are of great relevance, as they can provide objective and near real-time HAT identification.

3.1. **Method using Columnar and Surface (C&S) aerosol data: C&S inventory**

One of the HAT inventories used in this study follows the methodology described by Cachorro et al. (2016) for the identification of mineral dust intrusions. The methodology used in that study serves as a reference for the other methodologies. It is based on the joint interpretation of columnar (AOD, AE) and surface data (PM_{10}), making the visual inspection of the whole time series of instantaneous values with predefined threshold values. Obviously, the procedure is hard and time consuming, similarly in this aspect to the SPR method. The advantage of the simultaneous usage of columnar and surface aerosol quantities is that they contain complementary information which can help to identify and classify a HAT event day even if a HAT fingerprint is absent or very weak in one of the two data sets. Furthermore, the impact of missing one data type on a certain period is minimized since the other data can still be analyzed. Besides, in order to ensure the reliability of the HAT event, ancillary information is also required.

Due to the clean continental conditions of our study area, moderate and high intensity episodes can be detected by establishing certain AOD_{DS} thresholds at 440nm wavelength ($AOD_{DS,440nm}$) and in terms of PM_{10}. Instantaneous values of $AOD_{DS,440nm}$ and AE_{DS} are used for the detection of high turbidity events, together with the daily concentrations of PM_{10}. The HAT episodes are defined as those cases showing an aerosol load of $AOD_{DS,440nm} \geq 0.18$ and/or $PM_{10} \geq 13$ $\mu g/m^3$ (Cachorro et al., 2016). These thresholds were established based on the analysis of aerosol climatology (both $AOD_{DS,440nm}$ and PM_{10}) and previous knowledge about the aerosols over this area (e.g., Bennouna et al., 2013; 2016; Burgos et al., 2016).

The discrimination between fine or coarse particles causing the high turbidity is defined in terms of AE_{DS} parameter. The $AE_{DS} < 1.0$ is taken to identify desert dust events ('D' flag) and $AE_{DS} \geq 1.5$ to represent urban-industrial and biomass burning pollution ('A' flag). The interval of $1.0 < AE_{DS} < 1.5$ is taken to represent mixtures, either labelled as 'MD' or 'MA' according to the available ancillary information.

The classification of each day of each event is corroborated by analyzing ancillary information (a process which is also very beneficial in helping to determine the duration of the events). This ancillary information is, mainly: HYSPLIT backward air mass trajectories, MODIS RGB and AOD images,

meteorological maps and the NAAPS Global Aerosol model (Navy Aerosol Analysis and Prediction System). Further details about this method were described in detail by Cachorro et al. (2016). The used ancillary information for this method and SPR method is very similar.

The C&S inventory includes 667 HAT event days in the 2005-2014 period (18% of the days). A total of 330 are categorized as dust days, with 193 in the "D" category and the rest (137) in the "MD" category . A total of 189 and 148 event days were, respectively, attributed to the 'A' and 'MA' categories.

3.2. **Method using Spectral Deconvolution Algorithm (SDA): SDA inventory**

3.2.1. First step in the identification of fine and coarse mode HAT episodes

Products derived from Spectral Deconvolution Algorithm are based on the spectral curvature of the AOD values. This information, represented by its spectral derivatives, α and α', is essential to extracting the fine and coarse mode components of the AOD. . The bimodal basis for spectral curvature analysis can be found in O'Neill et al. (2001) while the fine/coarse mode retrieval algorithm (the Spectral Deconvolution Algorithm or SDA) was described by O'Neill et al. (2003). The SDA retrievals of fine mode AOD (AOD_F) and coarse mode AOD (AOD_C) along with the corresponding fine mode AOD fraction (η) at 500nm wavelength, are an operational AERONET product.

The AOD_F and AOD_C time series for the entire data set were analysed in detail (e.g., frequency histograms are shown in Figure S1). A systematic statistical analysis leads us to propose the 85^{th} percentile (P85) as an indicator of high atmospheric turbidity episodes associated with each mode. An AOD_F value exceeding 0.12 (P85 of AOD_F) is labelled as fine mode aerosol event (first flag 'F'). If the AOD_C value is larger than 0.05 (P85 of AOD_C) the event is declared to be coarse in nature (first flag 'C'). If both flags of each individual mode are activated, then the event is labelled as an aerosol mixture ('M' flag). To sum up:

- If $AOD_C \geq (P85)_C$: 'C' flag (coarse event)
- If $AOD_F \geq (P85)_F$: 'F' flag (fine event)
- If $AOD_C > (P85)_C$ & $AOD_F > (P85)_F$: 'M' flag (mixture event)
- If $AOD_C < (P85)_C$ & $AOD_F < (P85)_F$: 'NT' flag (non-turbid)

where $(P85)_{C/F}$ is the corresponding percentile for the coarse(C)/fine(F) AOD at 500nm wavelength.

The use of an 85^{th} percentile is, an appropriate way of objectively adapting our HAT threshold approach to local or regional conditions. Given that this inventory is generated by using SDA retrievals, it is

labelled the 'SDA' inventory. This method, therefore, only uses AOD_F and AOD_C data. In order to check the aerosol type identification the α' vs α space is used, which is also defined by SDA products. This approach is rendered more informative if one contextualizes the aerosol classification with families of fine mode fraction (η) and spectral curvature parameter ('t') curves (see the definition of "t" given by O'Neill, 2001). The 't' values are related to the fine mode aerosol type and independent of η (independent of the aerosol content as per O'Neill, 2010). Furthermore, it provides a visible tool that helps to better understand how a certain aerosol type interacts with the local environment. This kind of diagram, overlaid by the continuously differentiable (η, t) family of curves is a graphical representation of the curvature implications of bi-modality. Figure 1a shows an α' vs α scatterplot with the superimposed curves of constant η and 't' for the different classes of HAT event days ('C', 'F', and 'M' categories) at the Palencia site. Most HAT conditions in the coarse mode present negative α' values and η below 0.7. With respect to 'F' event days, they are placed in the upper region of the plot: $\eta \geq 0.7$ and positive α', with most of the 't' values between -0.47 and 1.39. The mixture aerosol type occupies a large region ($0.2 < \eta < 0.8$) and with most of the 't' values being in the neighborhood of the t=1.39 curve. Therefore, the three aerosol types in our classification by SDA method can be identified in the α' vs α space.

Different case studies have been reported for α' vs α diagrams. O'Neill (2010), for instance, presented a coarse mode event at the CARTEL AERONET (AEROCAN) site with η values below 0.7 and 't' parameter values confined between 1.39 and 2.15, while a fine mode event was located in the region for which $\eta \geq 0.7$ and 't' values were between 0.55 and 2.15. In a pristine sub-Arctic area, Rodríguez et al. (2012) found that continental and smoke/pollution episodes were located in the upper region of this kind of diagram ($\eta > 0.7$ and 't' values between -0.47 and 2.15) while marine aerosols were located in the $\eta < 0.7$ region. Spectral pairs in the upper (high η) regions of α' versus α plot were also reported by Salinas et al. (2013) for a smoke event in Singapore. The value of $\eta = 0.7$ is somewhat a natural threshold between coarse and fine mode HAT event days. In fact, this value was used to discriminate between different types of mixed classes for HAT episodes that were classified as mixtures (as performed in the next subsection).

Our SDA classification approach (flags of 'F', 'C', and 'M') yields similar classification categories to those of previous studies (e.g., O'Neill, 2010; Rodríguez et al., 2012; Salinas et al., 2013).A total of 641 HAT event days in the period 2005-2014 were identified with this method. There are 297 (46%) event days with HAT in the coarse mode ('C' flag), 233 (37%) in the fine mode ('F' flag), and 111 (17%) simultaneously presenting HAT in both modes ('M' flag).

3.2.2. Identification of ‘D’, ‘MD’, ‘A’, and ‘MA’ categories.

Once ‘C’,‘F’ and ‘M’ aerosol types are identified, we need to ensure the source of the aerosol particles if the SDA algorithm is to be compared with the previous C&S inventory. In addition, the mixture predominant types (‘MA’ or ‘MD’) can be identified too.

Therefore we added air mass back-trajectory information to the a-priori resulting inventory. Paths followed by air mass trajectories were determined using the HSPYLIT model (see Section 2.2). Possible aerosol sources on the African, European, and American continents as well as local areas were determined for each activated flag. If the first flag is ‘C’, air masses crossing the African Continent are searched. If the path followed (at any height) crosses Africa, at least 15% of the entire back-trajectory (see Section 2.2), the aerosol source for this air mass is attributed to North African (Saharan and Sahel) deserts. The presence of coarse particles is then attributed to mineral dust and the final flag is set to ‘D’. This kind of methodology has been employed by previous studies on the Iberian Peninsula (e.g., Toledano et al., 2009; Mateos et al., 2015; Cabello et al., 2016). If the first flag is ‘F’ and the air masses spent at least 15% of their flight time over the European and American Continents (or in the local area), then the fine mode nature of the event is reinforced. Pollution resulting from fine mode aerosols (‘A’ aerosol type) is then identified with the final flag of ‘A’ replacing the ‘F’ flag.

Possible sources are also checked for the mixture conditions associated with the first flag ‘M’. Those cases set to the ‘M’ flag along with an aerosol source in North Africa and showing values of $\eta \leq 0.7$ are interpreted as mixture conditions but with a predominant desert dust contribution (see Figure 1a): their final flag is accordingly set to ‘MD’ (mixtures with desert dust). If the ‘M’ flag occurs simultaneously with a fine mode fraction above 0.7, aerosol sources over the American and European continents and local areas are searched. If one of those areas is determined to be the source the final flag for those cases is ‘MA’ (mixtures with a predominance of fine mode particles).

The main characteristics for the (α, α') space in the first step (HAT identification, Figure 1a) are essentially conserved in Figure 1b: the ‘D’ classes remain in the ‘C’ and ‘M’ regions and the ‘A’ classes remain in the ‘F’ and ‘M’ regions.

With the more restrictive aerosol type classification criteria of the second step, the number of event days has been slightly reduced from 641 to 538 (loss of 103 days). These 538 days of high turbidity are, respectively, sub-classified, into 205, 58, 232, and 43 occurrences of the ‘D’, ‘MD’, ‘A’, and ‘MA’ flags.

The 103 high turbidity days with no clear air mass trajectory were further studied. A total of 90 out of those 103 event days indicate the presence of coarse particles. This is not directly attributed to air masses crossing over from North Africa, and therefore, they are not classified as 'D'. They retain the 'C' flag (high turbidity in the coarse mode) but are not analysed in this study and do not appear in Figure 1b. These events exceed the nominal HAT conditions for the coarse mode (P85 $AOD_C > 0.05$) but they do not correspond to very large AOD_{500}. For all these 90 cases, the median yielded a value of 0.14. This figure is smaller than the corresponding value obtained for the 'D' category: 0.19. Only 3 event days, initially classified as fine mode HAT episodes, did not meet the air mass criterion and accordingly retained the 'F' flag: these events are not analysed in this study and do not appear in Figure 1b. Finally, 10 event days showing mixture conditions could not, because of the air mass trajectories, be classified as 'MD' or 'MA' and they are omitted in this study.

The result of this automatic algorithm is accordingly the identification and classification of HAT event days when air mass back-trajectory supports the presence of coarse mode dust 'D' or fine mode 'A' aerosol types.

We must call attention that there are event days which are difficult to classify because instantaneous AOD/AE (or AOD_C, AOD_F) values present low or very variable intensity ranging in the edges of the threshold values. An entire day (not instantaneous data) is assigned to an aerosol type, therefore additional information is needed in such cases.

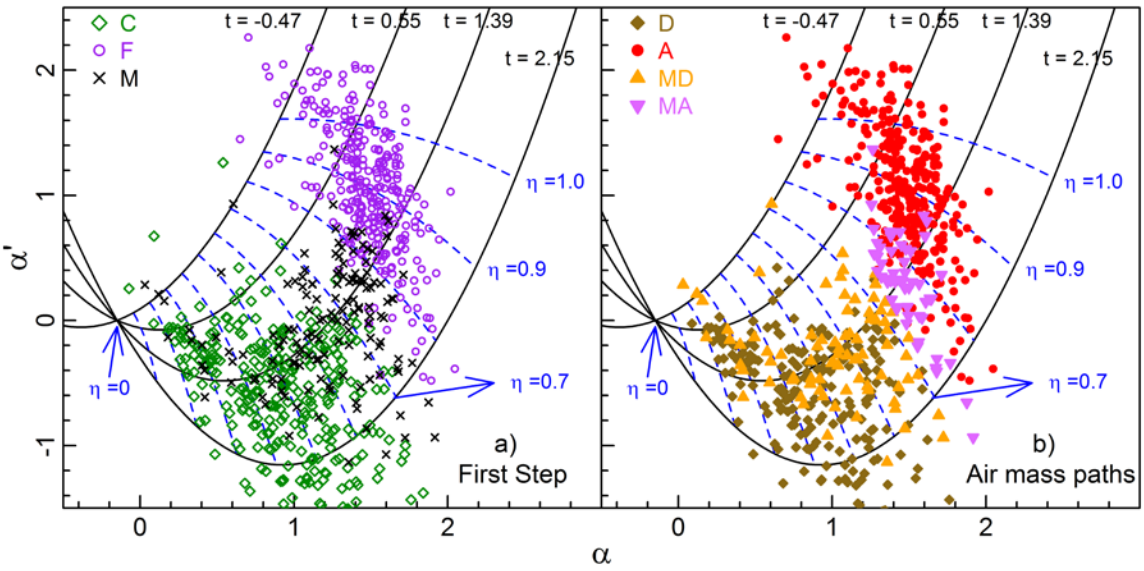

Figure 1. Scatterplots of α' vs α (at 500 nm from SDA algorithm) for different aerosol types: (a) simple classification (three different flags) using the scheme of Section 3.2.1 and (b) classification scheme of Section 3.2.2 considering air mass paths (four different flags). Curvilinear coordinate curves of constant 't' and η are superimposed on the graph (c.f. O'Neill, 2010). These classifications were applied to the entire 2003 to 2014 AERONET database of Table 1.

3.3. **Spanish and Portuguese Reference (SPR) method: SPR inventory**

The third methodology used for identifying HAT episodes has been extensively reported (Escudero et al., 2005, 2007; Querol et al., 2009; Viana et al., 2010). It is related to surface PM_{10} data and has been successfully applied to identify African dust outbreaks in particular. . This procedure largely assures the identification of African dust episodes, independently of their intensity: it involves the joint interpretation of meteorological products, aerosol maps from model forecasts, satellite imagery and air mass back-trajectories. This inventory also allows for possible time delays of up to 2 days in PM_{10} levels after the desert dust intrusion (Pey el al., 2013). This inventory is yearly reported by the Spanish Government (http://www.mapama.gob.es/es/calidad-y-evaluacion-ambiental/temas/atmosfera-y-calidad-del-aire/calidad-del-aire/evaluacion-datos/fuentes-naturales/) in order to assess the natural contribution to excessive PM_{10} concentrations in different sectors of the Iberian Peninsula (Pérez et al., 2018). The European Commission (EC) has adopted this method as the standard for investigating the role of desert dust intrusions over the whole continent (e.g., EC, 2010). The name attributed to this inventory is SPR (the Spanish-Portuguese reference method, following Viana et al., 2010). Among all the available sectors, we concluded the northern sector is the most suitable for the comparison in this study. The

northern Iberian Peninsula inventory associated with this third methodology was accordingly downloaded and analysed. A total of 334 dusty days were identified during the 2005-2014 period.

The SPR methodology also determines the episodes of type "A" but these episodes are not based on experimental data, therefore they were not considered in this study for this method. Preliminary results have shown a notable underestimation in the identification of 'A' pollution episodes when this methodology is compared with the previous two methods.

4. Comparison of the three different methodologies

4.1.Comparison of detected HAT episodes (2005 – 2014)

The yearly number of 'D' and 'A' event days identified by the three inventories described in Section 3 are shown in Figure 2. Those days with 'MD' and 'MA' flags are also added in the bar plots of C&S and SDA methods. Overall, the number of 'D' and 'A' event days can range, with some exceptions, between 20 and 40 per year. There is no correlation between the year to year time series of 'D' and 'A' event days, therefore showing a great variability. The number of dusty days per year in Figure 2a shows that the SPR inventory results in more event days than the other two methods. It also shows year 2007 as the one with the largest number of desert dust event days (about 60). The three inventories show 2013 to be the year with the minimum number of desert dust outbreaks (less than 8 days). The largest 'D'+'MD' discrepancy between the SDA and the C&S methodology occurs in 2006. However, as pointed out by Cachorro et al. (2016), no columnar data are available in June and July of that year. The PM_{10} data in their C&S inventory, enabled the identification of 14 'D' event days along with 13 and 15 'MD' and 'MA' days, respectively.

Concerning the fine mode HAT (Figure 2b), the C&S and SDA inventories show good agreement with respect to 'A'+'MA' events.. These two inventories disagree in the identification of the 'MA' category in 2006 (because of the same reasonexplained above in terms of the lack of columnar data) and in 2009. The 'A'+'MA' time series generally behave in a similar relative way in terms of year to year variability. For 2007 and 2013, there are 'A' event days identified by SDA method which are detected as 'MA' by the C&S analysis, but this fact does not introduce significant discrepancy.

The total counts of 'D'+'MD' across the 2005 to 2014 period are 330, 263, and 334 for the C&S, SDA, and SPR inventories, respectively. These numbers indicate, therefore, a mean dusty days ('D'+'MD') occurrence of about 7-9% per year. This is in line with previous studies in the same region (e.g.,

Cachorro et al., 2016). A similar range of occurrence is found for 'A'+'MA' event days with a total count of 337 and 275 using C&S and SDA inventories, respectively (7.5-9% of the days).

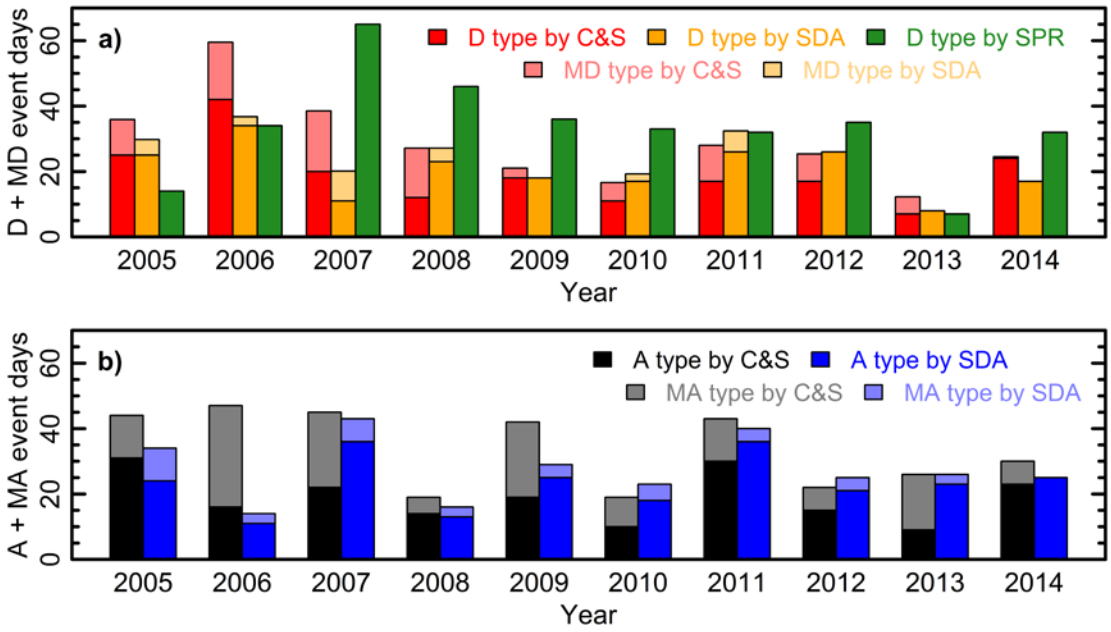

Figure 2. Evolution of the number of 'D' + 'MD' event days (a) for the three inventories used in this study, and 'A' + 'MA' event days (b) for the C&S and SDA inventories between 2005 and 2014.

Overall, there were 67 days of HAT conditions per year in the north-central Iberian Peninsula with roughly the same number of 'D' and 'A' event days. Saharan dust, in the context of unusually high aerosol loads in the western Mediterranean Basin (e.g. Pey et al., 2013; Gkikas et al., 2013) is responsible for the majority of the strongest aerosol episodes (e.g., Gkikas et al., 2016b). However, when a broader analysis of the variability of HAT event day intensity is performed, the roles of both 'D' and 'A' categories are more balanced.

Tables 1 and 2 show detailed comparisons of the three inventories for the four episode types, where the C&S inventory is considered as reference. When a 'D' or 'A' event day in one inventory is classified in the other inventory as one of the two mixture categories ('MD' or 'MA'), both inventories are considered to agree in the identification of HAT conditions. These labelling differences can be understood since the interpretation of the different aerosol properties using differing criteria can lead to different choices about the predominant type in each aerosol mixture.

The general agreement for those mineral dust outbreaks ('D'+'MD' type) in the SDA vs C&S and SPR vs C&S is above 60% and 50%, respectively. The SDA and SPR methods failed to categorize 67 and 71

dusty days identified by C&S while identifies 106 and 212 'D' flags, respectively, which are not in the C&S inventory (c.f. Tables 1 and 2 for more details). The SDA inventory missed 59 of the 67 dusty days because of the lack of columnar data (mostly in 2006, as mentioned above). The other 8 cases correspond to a lack of SDA retrieval data (2 days), no clear identification of air mass trajectory (2 days), and days in the beginning/ending of particular episodes (which were attributed to the 'D' type during the C&S visual inspection of instantaneous values) with an AOD_C below the threshold (4 days). In the SPR vs C&S comparison, the SPR method failed to identify 71 'D' event days. On 2 days SPR had no data (statistically negligible over 10 years).). The other 69 days were characterized by mean values of $PM_{10} = 21 \pm 16$ μg/m^3 and $AOD_{DS,440nm} = 0.27 \pm 0.12$.

The comparison of 'D' results was also performed at different $AOD_{DS,440nm}$ and PM_{10} intervals in order to investigate if the discrepancies/similarities between inventories could be better understood by employing stratified criteria (only the subset of 'D' days for which both $AOD_{DS,440nm}$ and PM_{10} data were available are analysed here). The SDA vs C&S comparison yielded perfect agreement (100% classification accuracy) for strong intrusions. These are defined by the mean + 2 standard deviations of the dataset (Bennouna et al., 2016): $AOD_{DS,440nm} > 0.3$ and $PM_{10} > 28$ μg m^{-3}. . There is a source of discrepancy between them, however, for desert dust intrusions associated with weaker AODs / mass concentrations ($AOD_{DS,440nm} < 0.3$ and $PM_{10} < 28$ μg m^{-3}). About 8% of the C&S 'D' event days are not identified by the SDA in this $AOD_{DS,440nm}$ /PM_{10} range (the classification match is nevertheless 92%). It is worth noting that detection of weak to moderate intensity episodes is very difficult since the dust fingerprint can be masked. The SPR vs C&S comparison shows perfect agreement for the strongest intrusions ($AOD_{DS,440nm} > 0.5$ and $PM_{10} > 28$ μg m^{-3}), but the identification of dusty days is problematic even for cases with large $AOD_{DS,440nm}$ (> 0.3) because they show $PM_{10} < 28$ μg m^{-3}. About 30% of the total dusty days included in the C&S inventory are not identified by the SPR method in these $AOD_{DS,440nm}$ and PM_{10} ranges.

It is remarkable that the large number of 'D' event days not in the C&S reference inventory but identified by the SDA and SPR methods (Tables 1 and 2) are characterized by relatively low aerosol loads. These days, therefore, do not have important impact on the determination of the dust contribution to the total load (in AOD or PM_{10}). The 106 dusty days added by the SDA method are characterized by mean $PM_{10} = 12 \pm 7$ μg/m^3 and $AOD_{DS,440nm} = 0.15 \pm 0.03$ ($AE_{DS} = 0.8 \pm 0.2$) while the mean for the 212 dusty days added by the SPR method are $PM_{10} = 12 \pm 7$ μg/m^3 and $AOD_{DS,440nm} = 0.13 \pm 0.05$ ($AE_{DS} = 1.1 \pm 0.4$). For a particular case of low aerosol load, November 15th, 2012 with $PM_{10} = 8$ μg/m^3, $AOD_{DS,440nm} = 0.15$ ($AE_{DS} = 0.62$), and the SDA retrievals at 500nm $AOD_F = 0.043$ and $AOD_C = 0.064$. These conditions are non-high turbidity in the C&S and SPR inventories. But the AOD value in the

coarse mode is larger than the threshold for HAT conditions in the SDA inventory and this day is classified as 'D' because of the air mass trajectories. This kind of discrepancies do not occur for intense episodes, but the identification of those event days with moderate to low intensity can differ depending on the followed method or the measurement technique.

Table 1. Comparison of HAT event days identified using the C&S methodology with those using the SDA method (2005-2014 period). The classification (categorization) accuracy for HAT event days common to the C&S and SDA inventories is the "Categorized as" column entry: highlighted in bold font those categories that can be interpreted as good agreement.

Category in C&S	Total C&S	Category in SDA				
		D	MD	A	MA	No event
D	193	**99**	**26**	1	0	67
MD	137	**29**	**24**	23	**21**	40
A	189	0	0	**127**	**5**	57
MA	148	10	**6**	**47**	**16**	69
No event	2985	67	2	34	1	**2881**
Total SDA		205	58	232	43	3114

Table 2. Comparison of HAT event days identified using the C&S methodology with those using the SPR method (2005-2014 period). The classification (categorization) accuracy for HAT event days common to the C&S and SPR inventories is the "Categorized as" column entry: highlighted in bold font those categories that can be interpreted as good agreement.

Category in C&S	Total C&S	Category in SPR		
		D	MD	No event
D	193	**122**	**-**	71
MD	137	**47**	**-**	90
No event	2985	212	-	**2773**
Total SPR		381	-	2934

With respect to 'A' flags, the general agreement between the C&S and SDA methods is about 70%, but the SDA identifies 105 event days that are not in C&S. Six out of 57 unidentified 'A' event days are due to the lack of columnar data. A total of 29 days out of the remaining 51 event days show an AOD_F value very close to the established threshold (i.e. their values are found to be in the 0.10-0.12 interval). The 51 unidentified 'A' event days represent AOD_F values between the first and third quartile (0.077 and 0.114, respectively). Therefore, the AOD_F is relatively low compared to the P85 threshold, but the instantaneous $AOD_{DS,440nm}$ can display a larger value that can be considered as HAT conditions when the C&S visual inspection is carried out. This comparison was also carried out for the above-mentioned PM_{10} and $AOD_{DS,440nm}$ intervals, for those days with both types of data being available. As in the case of the 'D' category results, there was a very good agreement of 95% for the strong episodes ($AOD_{DS,440nm} > 0.3$ and $PM_{10} > 28$ μg m^{-3}). For moderate episodes ($AOD_{DS,440nm} < 0.3$ and $PM_{10} < 28$ μg m^{-3}), about 25% of the 'A' event days in C&S are not identified by the SDA method.. Most of the discrepancies (unidentified days) are observed at the beginning/ending of each event when the impact on aerosol load is weak. A visual inspection of these particular days showed 2 long-lasting episodes, of about 3-4 consecutive days each, as the only major discrepancies between the inventories. The AOD_F values during these days were slightly smaller than the required SDA HAT threshold. The large number of 'A' event days identified by the SDA and not in C&S are not characterized by high aerosol load levels ($PM_{10} = 10 \pm 3$ μg/m^3, $AOD_{DS,440nm} = 0.21 \pm 0.07$, and $AE_{DS} = 1.6 \pm 0.2$) and they present a minor impact on the determination of the 'A' contribution to the total aerosol load.

When there is availability of columnar AOD data, the automatic SDA method can provide reliable identification of HAT event days for 'D' and 'A' aerosol types. However, if there is a lack of AOD columnar data, the surface aerosol load should be taken into account in order to have a reliable inventory. The use of only surface data (together with ancillary information) presents some uncertainties for strong turbidity episodes, because long-range transported aerosol can remain in high tropospheric layers and have low impact at the surface, and hence a time lag (one or two days) is required for sedimentation process and thus for increasing PM_{10} values.

4.2. Case Study: example of the year 2014

In order to better show how the three methodologies work, particular examples of 'D', 'MD', 'A', and 'MA' event days that occurred in 2014 are shown in Figure 3. This year was selected because it presents moderate occurrence of HAT days, with a minor incidence of 'MD' episodes and it is illustrative of the problems encountered in this comparative analysis.

With respect to desert dust outbreaks, three long events (lasting more than three days in April, October and November) and a total of 24 dusty days are identified in the C&S inventory. A smaller number (a total of 17) is found in the SDA inventory. With respect to the SPR inventory, its total of 31 dusty days is notably augmented compared with the C&S counts by a particularly long episode (11-17 April 2014). This episode is a good illustration of the challenges associated with the discrepancies that can result from the different HAT categorization schemes. The episode is not identified in the same way by the other algorithms, where only two days (12-13 April 2014) are flagged as 'MA' category for C&S while the SDA flagged one 'D' and one 'A' category. However, as it can be observed in Figure 3, the beginning of this period is identified as a dusty day by both C&S and SDA inventories (4 October 2014: AOD_C=0.10 and PM_{10} = 17 $\mu g/m^3$). The columnar aerosol load for this long episode can only be considered as "high turbidity" on the two days mentioned before (12-13 April 2014), while the surface PM_{10} concentrations on those two days were low (between 9 and 12 $\mu g/m^3$).

The three algorithms simultaneously agree in the identification of HAT mineral dust events in 12 out of 24 C&S 'D' flags in 2014. One possible reason behind this relatively low classification match could be the weak intensity of desert dust outbreaks for this year with mean (median/maximum) $AOD_{DS,440nm}$ and PM_{10} values of 0.18 (0.16/0.35) and 24 (21/42) $\mu g/m^3$, respectively. The use of fixed and automatic thresholds can underestimate the frequency of mineral dust identification. However, this shortcoming is relatively minor since the analysis of ancillary information is the key that leads to the identification of desert dust aerosols for low intensity events.

An unusual and long period of high turbidity occurred between 23rd and 30th October, 2014. A visual inspection of all the available information associated with this extended desert dust event gives a global perspective (C&S and SPR) while the automatic algorithm (SDA) only identifies certain days. The days classified in the 'D' category by the C&S method but not identified by the SDA are those days with no available columnar data (e.g., cloudy conditions throughout the day) so that the C&S classification was carried out using only PM_{10} values. Although the month of October was not, within the context of a multi-year perspective, affected by a large number of desert dust intrusions over our study region (Cachorro et al., 2016), it does represent a monthly maximum of dusty days for 2014 with 11 'D' event days plus one 'MD' (as per the C&S method). The aerosol load levels during this month ranged between 0.09 and 0.27 for $AOD_{DS,440nm}$ and between 18 and 42 $\mu g/m^3$ for PM_{10}.

The C&S identification of urban-industrial and biomass burning in 2014 indicated 23 'A' days (plus 7 'MA' days), while 25 'A' days were identified using the SDA method. These two inventories have 21 'A'+ 'MA' episodic days in common. For instance, the 'A' flag reported by C&S on July 4th, 2014 is not corroborated by SDA method (although, we would point out that the AOD_F value is very close to the HAT threshold; AOD_F = 0.115, the P85 threshold is 0.12). The identification of 'A' event days by using only surface data seems problematic because of the weaker impact of this kind of fine particle events on PM_{10},as mentioned above. For instance, during all 'A' and 'MA' events of 2014 the maximum PM_{10} concentration is 22 $\mu g\ m^{-3}$, while the maximum $AOD_{DS,440nm}$ is 0.36. This emphasizes the different sensitivities of $AOD_{DS,440nm}$ and PM_{10} to the detection of desert and 'A' episodes (e.g., Cabello et al., 2016).

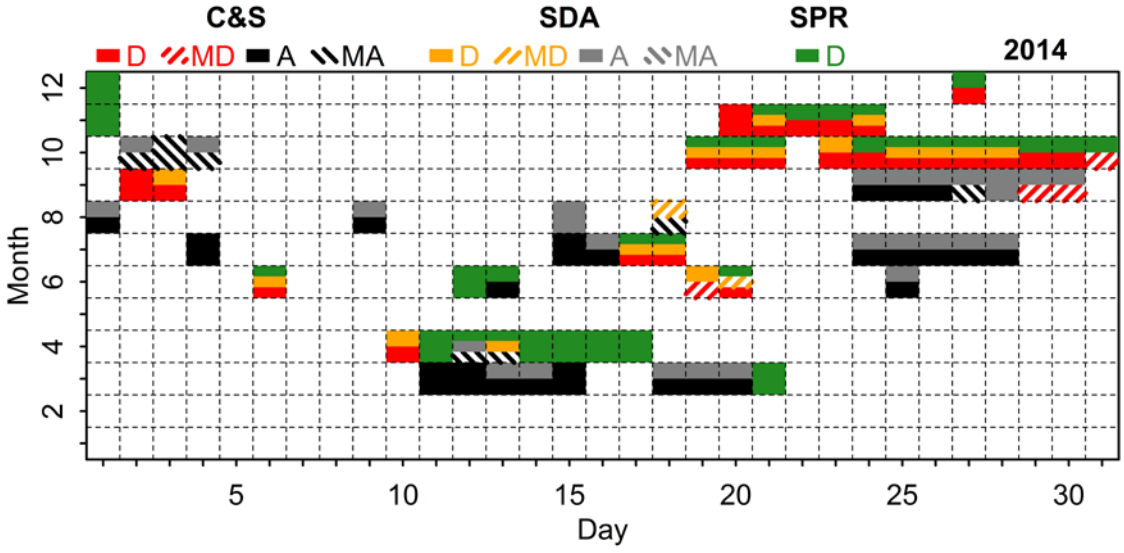

Figure 3. Inventory of 'D', 'MD', 'A', and 'MA' event days in 2014 identified by three different methodologies.

4.3. Sensitivity of using 85th percentile in the SDA method

The application of 85th percentiles to SDA-derived AOD_C and AOD_F values has proven to be a good tool for high turbidity identification. One might ask whether the use of other percentiles could also lead to a reliable means of identifying aerosol episodes. In this section, the sensitivity of the proposed percentile methodology is accordingly studied. The 80th, 85th, and 90th percentiles are chosen for this sensitivity test of high turbidity identification. Table 3 presents the values of the corresponding thresholds applied to the Palencia database for the 2005-2014 period.

Table 3. 80th to 90th percentiles for AOD_F and AOD_C series for 'Palencia' AERONET site database (2005-2014 period).

Percentile	AOD_F	AOD_C
80th	0.10	0.04
85th	0.12	0.05
90th	0.15	0.07

The methodology for this test is the same as explained above (see Section 3.2.1). Bear in mind that only data of AOD_C and AOD_F are necessary to identify 'C', 'F', and 'M' categories, first step of SDA inventory.

The results of the HAT identification using 80th, 85th, and 90th percentiles are compared in Figure 4 with the 'C&S' identification method (considered as reference). The 90th percentile threshold exhibits the best agreement (81% of coincidence) between C&S and SDA inventories in the 'D' vs 'D' comparison. The use of 85th and 80th percentiles reduces the agreement in the 'D' vs 'D' case but notably increases the 'D' vs 'M' case with a total agreement of 94-96% for this type of episodes.

With respect to the fine-mode dominated cases, little change is observed by changing from 80th to 85th percentile thresholds with an agreement about 70% in the 'A' vs 'A' comparison. The use of 80th percentile identifies a larger number of 'A' event days in the 'M' category which are attributed to non-turbid ('NT' flag) cases with the use of the 85th percentile. All these cases are associated to values close the thresholds (between 0.10 and 0.12, see Table 3). The agreement is notably smaller for the 90th percentile analysis. Accordingly, the use of a large threshold (90th percentile), results in weaker events (AOD < 0.15) being misclassified as 'NT' category.

The two aerosol mixture categories ‘MD’ and ‘MA’ present similar features with respect to the threshold variation. There is a high agreement with the SDA inventories using 80^{th} and 85^{th} percentiles: 91-88% and 93-74%, respectively. The use of the 90^{th} percentile reduces the percentage agreement to ~50%.

We assume that a day classified as a HAT event by the SDA (‘C’, ‘F’, or ‘M’) represents good agreement when it corresponds to a C&S classification of ‘D’, ‘MD’, ‘MA’, or ‘A’. The only SDA event days that get lost, in accounting for changes from one percentile to another, are those which are transferred to the ‘NT’ category. The use of 80^{th} percentile yields an 88-97% agreement range for the four categories of the C&S inventory (the “agreement” being the sum of the ‘D’, ‘M’, ‘A’ % values for each of the four categories). The lower limit of this range decreases moderately to 73% and the upper limit is 95% for 85^{th} percentile. The 90^{th} percentile yields minimum values for both the lower and upper bounds of the range (48-89%). The fact that the automatic SDA algorithm accepts more HAT event days with decreasing percentile can imply a larger uncertainty with significantly greater numbers of false positives. For instance, the “D” identification for the smaller percentile (80^{th} percentile) yields 245 HAT attributions. This number gets reduced to 145 and 58 for 85^{th} and 90^{th} percentile thresholds, respectively. The use of any one of the three percentiles as threshold can be justified depending on the objective of the study. For our purposes, the 85^{th} percentile was the most adequate option: this enables an acceptable balance between the assured identification of high intensity episodes and the inclusion of a moderate number of weak intensity episodes.

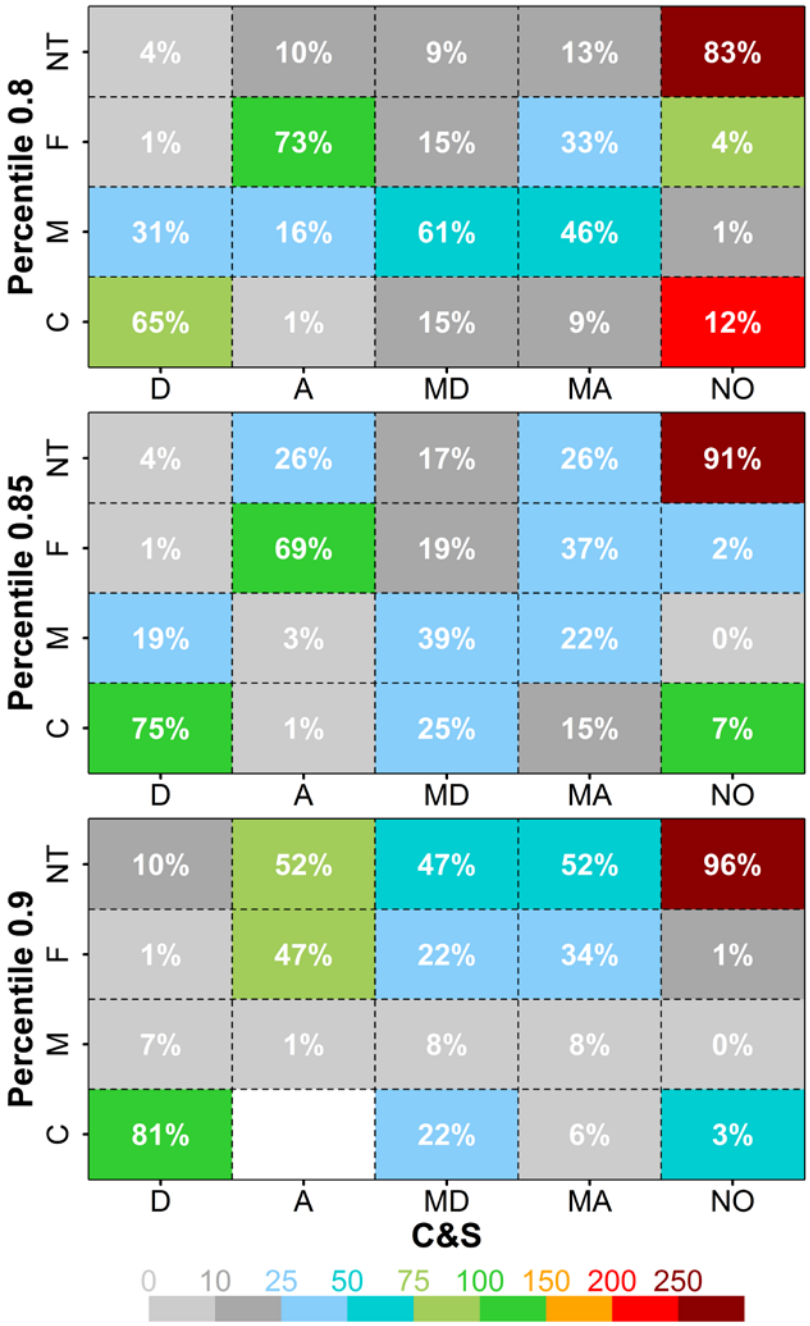

Figure 4. Identification of HAT episodes using the 'SDA' percentile method (80th, 85th and 90th percentiles; see text). The "C&S" inventory is used as reference. The colour scale quantifies the total number of identified HAT event days (values larger than 250 are saturated). The percentage agreement is given for each category (numbers in white text). The reader should keep in mind that, for each of the three percentile cases, the total number of events for a given C&S class is conserved (the sum of the superimposed percentages is 100% ± a rounding error).

5. Summary and Conclusions

To our knowledge, this is the first time that three aerosol inventories, dedicated to the identification and classification of high atmospheric turbidity events, have been compared. These inventories are based on different methodologies which make use of different types of aerosol data (columnar aerosol AOD data and surface PM_{10} data) while sharing similar ancillary information sources (air mass back-trajectory analysis, satellite imagery, aerosol models, etc.). The comparison is carried out for three aerosol types: coarse aerosol type, represented by mineral desert dust aerosol transported from the African continent; fine aerosol type, basically biomass burning aerosols from forest fires and anthropogenic aerosols transported from central Europe, the Mediterranean Basin or other regions of the Iberian Peninsula (long-range transported smoke from Canada has also been detected). A mixture of these two main aerosol types in the identified high atmospheric turbidity conditions was also investigated. Bear in mind that our region of study in the north-central Iberian Peninsula is a clean continental area.

The results of the comparison suggest that the simultaneous use of columnar (remote sensing) and surface (in situ) ground-based aerosol data provides the most reliable inventory. With this combined datasets, the impact of boundary layer to high-altitude atmospheric layers is taken into consideration given the high probability of at least one type of data being available: this capability eventually increases the probability of aerosol event detection. It is obvious that each aerosol database, columnar or surface, has its advantages and limitations. For instance, columnar aerosol data are based on direct sun irradiance measurements for which the sky must be cloud free in the direction of the sun: this results in significant duty cycle problems for cloudy sites. Conversely, PM_{10} measurements are not constrained by the sky conditions but do not allow the detection of events in the upper troposphere. The PM data analysis method requires a human observer to gather multiple information sources and its implementation in large areas with several sites can be very time consuming. This method can certainly be partially automated because it is mainly based on threshold values of physical measured/derived quantities, but initial results have shown that it is not as reliable as a measurement system supported by human observations, decisions and interpretations. Also, note that the implementation of the complementary information required for the identification of aerosol mixtures (MD or MA), is not an easy task because of the complex nature of the information and the decision process.

Given the drawbacks of all current existing methodologies, there are strong reasons to implement an inventory that is as automated as possible. The results of this study lead us to propose, as an alternative to the more labour intensive current approaches, an automated method based on the analysis of the fine and coarse mode AOD. The AOD_F and AOD_C parameters are found to be more powerful discriminators

than the combination of single wavelength AODs and alpha parameters. It can also be expected that classification methods based on thresholds applied to different variables may yield to different classifications, especially for weak events. The agreement has been shown to be nearly perfect for strong events.

The AOD_F and AOD_C are standard AERONET SDA products. The proposed approach permits the identification of high atmospheric turbidity (HAT) event days characterized as fine, coarse or mixed mode. This method requires the establishment of thresholds which serve as the basis for HAT identification. The results of this study led to the use of the 85^{th} percentile as a suitable threshold for both fine and coarse mode aerosol events. A sensitivity test to various thresholds demonstrated that significant changes in classification occurred only for event days with low AOD. Because HAT identification is primarily of concern in the presence of high AOD events, these low intensity cases have a minor impact. The proposed methodology can be readily adapted to near real-time HAT identification applied to the new AERONET Version 3.0 products. Those products incorporate improved cloud-screening capabilities that facilitate near-real-time data analysis. .

Acknowledgements

The authors are grateful to the Spanish Ministry of Science, Innovation and Universities for the support through the ePOLAAR project (RTI2018-097864-B-I00). Thanks are due to EMEP (especially to MAGRAMA and AEMET) and AERONET-PHOTONS- RIMA staff for providing observations and for the maintenance of the networks.

References

Bennouna, Y.S., Cachorro, V.E., Torres, B., Toledano, C., Berjón, A., de Frutos, A.M., Alonso-Fernandez Coppel , I. 2013. Atmospheric turbidity determined by the annual cycle of the aerosol optical depth over north-center Spain from ground (AERONET) and satellite (MODIS), Atmospheric Environment 67, 352-364.

Bennouna, Y.S., Cachorro, V.E., Mateos, D., Burgos, M.A., Toledano, C., Torres, B., de Frutos, A.M., 2016. Long-term comparative study of columnar and surface mass concentration aerosol properties in a background environment, Atmospheric Environment 140, 261-272.

Boucher, O., Randall, D, Artaxo, P., Bretherton, C., Feingold, G. , Forster, P., Kerminen, V. M., Kondo, Y., Liao, H., Lohmann, U., Rasch, P., Satheesh, S. K., Sherwood, S., Stevens, B. Zhang, X. Y., 2013. Clouds and aerosols, In: Climate Change 2013: The Physical Science Basis, Contribution of Working Group I to the Fifth Assessment Report of

the Intergovernmental Panel on Climate Change, [Stocker, T.F., D. Qin, G.-K. Plattner, M. Tignor, S.K. Allen, J. Boschung, A. Nauels, Y. Xia, V. Bex and P.M. Midgley (eds.)], 571-657, Cambridge University Press, Cambridge, United Kingdom and New York, NY, USA.

Burgos, M.A., Mateos, D., Cachorro, C., Toledano, C., de Frutos, A.M., 2016, Aerosol properties of mineral dust and its mixtures in a regional background of north-central Iberian Peninsula, Science of the Total Environment 572, 1005-1019.

Cabello, M., Orza, J.A.G., Dueñas, C., Liger, E., Gordo, E., Cañete, S., 2016, Back-trajectory analysis of African dust outbreaks at a coastal city in southern Spain: Selection of starting heights and assessment of African and concurrent Mediterranean contributions, Atmos. Env. 140, 10-21.

Cachorro, V. E., Burgos, M.A., Mateos, D., Toledano, C., Bennouna, Y., Torres, B., de Frutos, A.M., Herguedas, A., 2016. Inventory of African desert dust events in the North-central Iberian Peninsula in 2003-2014 based on Sun photometer and PMx data. Atmos Chem Phys. 16, 8227-8248. doi:10.5194/acp-16-8227-2016.

EC, 2010. Guidance on the quantification of the contribution of natural sources under the EU Air Quality Directive 2008/50/EC. Draft version 2, (presented to AQ Committee in June 2010); May 2010.

Escudero, M., Castillo, S., Querol, X., Avila, A., Alarcón, M., Viana, M. M., Alastuey, A., Cuevas, E., Rodríguez S., 2005. Wet and dry African dust episodes over eastern Spain. J. Geophys. Res. 110, D18S08. doi:10.1029/2004JD004731.

Escudero, M., Querol, X., Pey, J., Alastuey, A., Pérez, N., Ferreira, F., Alonso, S., Cuevas, E., 2007. A methodology for the quantification of the net African dust load in air quality monitoring networks. Atmos. Environ. 41(26), 5516-5524. doi: 10.1016/j.atmosenv.2007.04.047.

Giles, D.M., Sinyuk, A., Sorokin, M. G., Schafer, J. S., Smirnov, A., Slutsker, I., Eck, T. F., Holben, B. N., Lewis, J. R., Campbell, J. R., Welton, E. J., Korkin, S. V., Lyapustin, A. I., 2019. Advancements in the Aerosol Robotic Network (AERONET) Version 3 database – automated near-real-time quality control algorithm with improved cloud screening for Sun photometer aerosol optical depth (AOD) measurements. Atmos. Meas. Tech., 12, 169–209, https://doi.org/10.5194/amt-12-169-2019.

Gkikas, A., Hatzianastassiou, N., Mihalopoulos, N., Katsoulis, V., Kazadzis, S., Pey, J., Querol, X., Torres, O., 2013. The regime of intense desert dust episodes in the Mediterranean based on contemporary satellite observations and ground measurements, Atmos. Chem. Phys., 13, 12135–12154, doi:10.5194/acp-13-12135-2013.

Gkikas, A., Basart, S., Hatzianastassiou, N., Marinou, E., Amiridis, V., Kazadzis, S., Pey, J., Querol, X., Jorba, O., Gassó, S., Baldasano, J. M., 2016a. Mediterranean intense desert dust outbreaks and their vertical structure based on remote sensing data, Atmos. Chem. Phys., 16, 8609-8642, doi:10.5194/acp-16-8609-2016.

Gkikas, A., Hatzianastassiou, N., Mihalopoulos, N., Torres, O., 2016b. Characterization of aerosol episodes in the greater Mediterranean Sea area from satellite observations (2000-2007), Atmospheric Environment 128, 286-304.

Holben, B. N., Eck, T., Slutsker, I., Tanré, D., Buis, J. P., Setzer, A., Vermote, E., Smirnov, A., 1998. AERONET - A federated instrument network and data archive for aerosol characterization. Remote. Sens. Environ. 66(1), 1-16. doi: 10.1016/S0034-4257(98)00031-5.

Holben, B.N., D. Tanre, A. Smirnov, T.F. Eck, I. Slutsker, N. Abuhassan, W.W. Newcomb, J. Schafer, B. Chatenet, F. Lavenue, Y.J. Kaufman, J. Vande Castle, A. Setzer, B. Markham, D. Clark, R. Frouin, R. Halthore, A. Karnieli, N.T. O'Neill, C. Pietras, R.T. Pinker, K. Voss, and G. Zibordi.(2001), An emerging ground-based aerosol climatology: Aerosol Optical Depth from AERONET, J. Geophys. Res., 106, 12067-12097.

Levy, R.C., Remer, L.A., Kleidman, R.G., Mattoo, S., Ichoku, C., Kahn, R., Eck, T.F., 2010. Global evaluation of the Collection 5 MODIS dark-target aerosol products over land. Atmos. Chem. Phys. 10(21), 10399-10420.

Mateos, D., Cachorro, V. E., Toledano, C., Burgos, M. A., Bennouna, Y., Torres, B., Fuertes, D., González, R., Guirado, C., Calle, A., de Frutos, A.M., 2015. Columnar and surface aerosol load over the Iberian Peninsula establishing annual cycles, trends, and relationships in five geographical sectors, Sci. Total Environ., 518–519, 378–392, doi:10.1016/j.scitotenv.2015.03.002.

MITECO 2019; https://www.miteco.gob.es/es/calidad-y-evaluacion-ambiental/temas/atmosfera-y-calidad-del-aire/calidad-del-aire/evaluacion-datos/fuentes-naturales/anuales.aspx.

O'Neill, N.T., Dubovik, O., and Eck, T.F., 2001, Modified Ångström exponent for the characterization of submicrometer aerosols, Appl. Opt. 40, 2368-2375.

O'Neill, N.T., Eck, T.F., Smirnov, A., Holben B.N., Thulasiraman, S., 2003. Spectral discrimination of coarse and fine mode optical depth, J. Geophys. Res., 108(D17), 4559, doi:10.1029/2002JD002975.

O'Neill, N. T.: Comment on "Classification of aerosol properties derived from AERONET direct sun data" by Gobbi et al. (2007), Atmos. Chem. Phys., 10, 10017-10019, doi:10.5194/acp-10-10017-2010, 2010.

Pappalardo, G., Amodeo, A., Apituley, A., Comeron, A., Freudenthaler, V., Linné, H., Ansmann, A., Bösenberg, J., D'Amico, G., Mattis, I., Mona, L., Wandinger, U., Amiridis, V., Alados-Arboledas, L., Nicolae, D., and Wiegner, M.: EARLINET: towards an advanced sustainable European aerosol lidar network, Atmos. Meas. Tech., 7, 2389–2409, https://doi.org/10.5194/amt-7-2389-2014, 2014.

Pey, J., Querol, X., Alastuey, A., Forastiere, F., Stafoggia, M., 2013. African dust outbreaks over the Mediterranean Basin during 2001-2011: PM10 concentrations, phenomenology and trends, and its relation with synoptic and mesoscale meteorology, Atmos. Chem. Phys., 13(3), 1395-1410, doi:10.5194/acp-13-1395-2013.

Pérez, N., Querol, X., Alastuey, A., Olivares, I., Hervas, M., Cornide, M.J, Javato, R., Salvador, P., Artiñano, B., de la Rosa, J., 2018. Episodios naturales de partículas 2017. "CSIC, CIEMAT, Ministerio de Agricultura y Pesca, Alimentación y Medio Ambiente, Subdirección General de Calidad del Aire y Medio Ambiente Industrial". April 2018. See this report at web-page: https://www.miteco.gob.es/es/calidad-y-evaluacion-ambiental/temas/atmosfera-y-calidad-del-aire/calidad-del-aire/evaluacion-datos/fuentes-naturales/anuales.aspx.

Querol, X., Pey, J., Pandolfi, M., Alastuey, A., Cusack, M., Pérez, N., Moreno, T., Kleanthous, S., 2009. African dust contributions to mean ambient PM10 mass-levels across the Mediterranean Basin. Atmos. Environ. 43(28), 4266-4277, doi: 10.1016/j.atmosenv.2009.06.013.

Rodríguez, E., Toledano, C., Cachorro, V. E., Ortiz, P., Stebel, K., Berjón, A., Blindheim, S., Gausa, M. de Frutos, A. M. 2012. Aerosol characterization at the sub-Arctic site Andenes (69°N, 16°E), by the analysis of columnar optical properties. Q.J.R. Meteorol. Soc., 138: 471–482. doi: 10.1002/qj.921.

Salinas, S.V., Chew, B.N., Miettinen, J., Campbell, J.R., Welton, E.J., Reid, J.S., Yu, L.E., Liew, S.C., 2013. Physical and optical characteristics of the October 2010 haze event over Singapore: A photometric and lidar analysis. Atmospheric Research 122, 555-570, doi:10.1016/j.atmosres.2012.05.021.

Shifrin, K.S., 1995. Simple relationships for the Ångström parameter of disperse systems. Appl. Opt. 34, 4480-4485.

Stein, A.F., Draxler, R.R, Rolph, G.D., Stunder, B.J.B., Cohen, M.D., and Ngan, F., (2015). NOAA's HYSPLIT atmospheric transport and dispersion modeling system, Bull. Amer. Meteor. Soc., 96, 2059-2077.

Toledano, C., Cachorro, V. E., de Frutos, A. M., Sorribas, M., Prats, N., 2007. Inventory of African Desert Dust Events Over the Southwestern Iberian Peninsula in 2000–2005 with an AERONET Cimel Sun Photometer, J. Geophys. Res., 112, D21201, doi:10.1029/2006JD008307.

Toledano, C., Cachorro, V.E., de Frutos, A.M., Torres, B., Berjón, A., Sorribas, M., Stone, R.S., 2009. Airmass Classification and Analysis of Aerosol Types at El Arenosillo (Spain). J. Appl. Meteorol. Clim. 48, 962-981.

Valenzuela, A., Olmo, F. J., Lyamani, H., Antón, M., Quirantes, A., and Alados-Arboledas, L., 2012. Classification of aerosol radiative properties during African desert dust intrusions over southeastern Spain by sector origins and cluster analysis, J. Geophys. Res., 117, D06214, doi:10.1029/2011JD016885.

Viana, M., Salvador, P., Artiñano, B., Querol, X., Alastuey, A., Pey, J., Latz, A.J., Cabañas, M., Moreno, T., García, S., Herce, M., Diez, P., Romero, D., Fernández, R., 2010. Assessing the perfomance of methods to detect and quantify African dust in airborne particulates, Environ. Sci, Technol., 44, 8814-8820, doi: 10.1021/es1022625.

Vergaz, R., Cachorro, V.E., de Frutos, A.M., 2001. A quantitative comparison of alpha ångström turbidity parameter retrieved in different spectral ranges based on spectroradiometer solar radiation measurements. Atmos. Environ. 35, 5117-5124.

SUPLEMENTARY MATERIAL

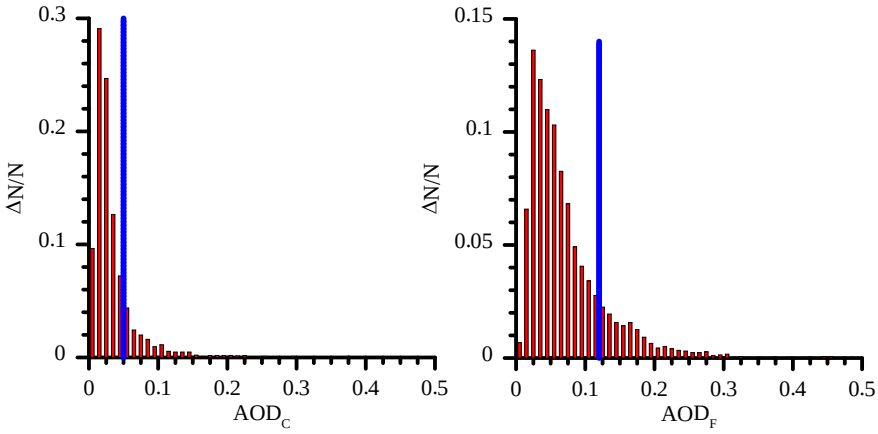

Figure S1. Histogram of AOD values for the coarse and fine modes at Palencia site. Vertical lines point out the P85 value used as threshold.